ELSEVIER

Coordination Chemistry Reviews 237 (2003) 135–146

COORDINATION CHEMISTRY REVIEWS

www.elsevier.com/locate/ccr

Vanadate chelate esters of monoionized diols and carbohydrates

Bharat Baruah [a], Samir Das [a], Animesh Chakravorty [a,b,*]

[a] *Department of Inorganic Chemistry, Indian Association for the Cultivation of Science, Kolkata 700 032, India*
[b] *Jawaharlal Nehru Centre for Advanced Scientific Research, Jakkur, Bangalore 560 064, India*

Received 25 January 2002; accepted 5 September 2002

Contents

Abstract

The title diols are ethane-1,2-diol (H_2ed), propane-1,3-diol (H_2pd), catechols (H_2Rcat) as well as glycerol (H_3pt) which act essentially as a substituted diol. The carbohydrates are methylated β-D-galactopyranoside (β-D-H_2gp), α-D-mannopyranoside (α-D-H_2mp) and β-D-ribofuranoside (β-D-H_2rf) and 4,6-benzylidine-α-D-mannopyranoside (α-D-H_2bmp), each of which have two vicinal hydroxyl groups having *cis* disposition. To achieve mononuclearity blocking of three coordination positions by tridentate ONO coordinating salicylaldimines (H_2Asal) of α-amino acids and hydrazones (H_2Abh) of benzyolacetone and salicyldehyde have been employed. Esters of type [VO(Hed)(Asal)], [VO(Hpd)(Asal)], [VO(H_2pt)(Asal)], [VO(β-D-Hgp)(Asal)], [VO(α-D-Hmp)(Asal)], [VO(β-D-Hrf)(Asal)], [VO(Hed)(Abh)], [VO(Hpd)(Abh)], [VO(α-D-Hbmp)(Abh)], [VO(HRcat)(Abh)] have been isolated and characterized. In general, the monoionized diols and carbohydrates are *O*,*O* chelated to the metal and the systems generally display hydrogen bonded association in the crystalline state. Species with chiral $Asal^{2-}$ ligands have exclusive *endo* configuration in the solid state, but in solution a sterically controlled *endo*–*exo* equilibrium prevails in the case of the aliphatic diol esters for which the ^{51}V chemical shift is also an index of chelate ring size. The carbohydrate esters do not display *endo*–*exo* isomerism in solution. Unlike the aliphatic systems the aromatic diol esters undergo spontaneous catecholase reaction with oxygen in solution, quantitatively affording the corresponding quinone. A catalytic cycle has been constructed for the reaction.

* Corresponding author. Tel.: +91-33-472-4436; fax: +91-33-473-2805
E-mail address: icac@mahendra.iacs.res.in (A. Chakravorty).

0010-8545/02/$ - see front matter © 2002 Elsevier Science B.V. All rights reserved.
PII: S0010-8545(02)00250-3

Keywords: Vanadate chelate esters; Vanadate esters of aliphatic diols and glycerol; Vanadate esters of modified carbohydrates; Diastereoisomeric equilibria in vanadate esters; Vanadate esters of catechols; Catecholase reaction

1. Introduction

It has been known for a long time that vanadium, like phosphorus, forms alkoxides or esters in the pentavalent state [1–3]. The essential functional entity of such species is $V^{V}O(OR)$ which was first structurally characterized in the methoxide, $[\{(VO(OMe)_3)_2\}_n]$, an alkoxide bridged polymer of dimers, the metal atoms being distorted octahedral [4]. More recently, dimeric esters such as $[\{VO(OCH_2CH_2Cl)_3\}_2]$ with pentacoordinated vanadium have been reported [5,6]. While alkoxide bridging appears to be a dominant structural feature, tetrahedral monomeric esters have also been observed in solution but X-ray structural characterization is lacking [7]. In summary, oxovanadium alkoxides can assume varied coordination geometries depending on the R group and physical conditions. The structural analogy between phosphate and vanadate esters is thus not perfect. But this comes with its own benefit—vanadates can represent transition state analogues of reactive phosphates [8]. This theme has found practical application in e.g. insulin mimicry [9,10]. The importance of vanadate ester chemistry is well recognized [11–13] and no further general reviewing will be done here.

The work concerning this article originated from the quest for mononuclear vanadate esters incorporating chelation by simple acyclic aliphatic diols. As progress was made, substituted carbohydrates and aromatic diols also become subjects of scrutiny. The synthesis structure and reactions of the new systems will be reviewed following a summary of work done by others on diol vanadates.

2. Ester chemistry of two aliphatic diols: a summary

The concerned diols are ethane-1,2-diol (H_2ed), **1** and propane-1,3-diol(H_2pd), **2**. The spontaneous esterification of H_2ed by vanadates in aqueous solution was first studied by ^{51}V-NMR spectroscopy [14]. A dimeric (presumably alkoxide-bridged) and chelated ester is the main solution constituent [15].

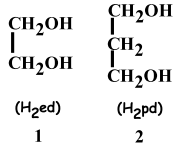

1 2

A few H_2ed esters have been isolated in the solid state [5,16,17]. The reaction of Li_2ed with $VOCl_3$ afforded light-yellow [VOCl(ed)] to which a tetrahedral geometry with chelated ed^{2-} was assigned on the basis of spectral data [5]. On the other hand, X-ray work on a colourless crystalline compound of the same composition but prepared by the reaction of $VOCl_3$ with $(SiMe_3)_2$ed revealed a dimeric structure, in which the ed^{2-} ligand does not chelate but bridges the VOCl fragments, the metal geometry being tetrahedral [16].

Solution studies on the esterification of H_2pd and other 1,3-diols have revealed that in no case does chelate formation occur [18,19]. The same applies to the solid compounds that have been isolated. Thus the reaction of LiHpd with $VOCl_3$ affords $[VOCl(Hpd)_2]$ in which Hpd^- is presumably coordinated to the metal at the alkoxide site only [5]. On the other hand, in the tetrameric complex $[\{VOCl(pd)\}_4]$, the pd^{2-} ligands act as bridges [20].

3. Mononuclear esters with chelation by Hed^-, Hpd^- and monoionized glycerol

3.1. Design strategy, synthesis and binding modes

The above state of development prompted us to undertake the task of designing mononuclear oxovanadium alkoxides incorporating chelation by H_2ed and H_2pd. To achieve this, the strategy [21–23] of blocking three of the oxovanadium coordination sites by an otherwise inert tridentate ligand leaving just two positions for possible diol chelation in an octahedral environment was employed.

The blocking ligands used [22,23] are of two types: salicylaldimines of α-amino acids, **3**, and hydrazones of benzoylacetone, **4**, and salicylaldehyde, **5**, abbreviated as

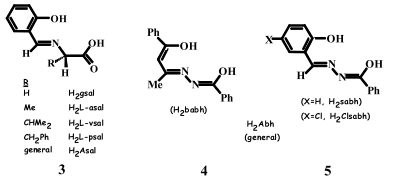

3 4 5

shown. In **3** the chiral (when R ≠ H) configuration of the amino acid residue is L. All the ligands are diacidic and potentially ONO coordinating.

The reaction of complexes of type $[V^{IV}O(Asal)(H_2O)]$ [23–26] with excess H_2ed in methanol under ambient conditions afforded deep-red solutions from which dark brown crystalline solids of composition $[V^{V}O(Hed)(A-$

sal)] were isolated in nearly quantitative yields [27,28]. Upon replacement of H_2ed by H_2pd in this preparative procedure, [V^VO(Hpd)(Asal)] is formed with equal ease [13]. To achieve H_2Abh-diol cochelation, $VO(acac)_2$ was reacted with H_2Abh in methanol–acetone mixture in air in the presence of a large excess of the diol. In this manner the dark coloured [V^VO(Hed)(Abh)] and [V^VO(Hpd)(Abh)] esters were isolated in high yields [29,30]. Success with H_2ed and H_2pd prompted us to scrutinize the behavior of propane-1,2,3-triol (H_3pt) i.e. glycerol **6** in the above reaction. Esters of type [V^VO(H_2pt)(Asal)] and [V^VO(H_2pt)(Abh)] were readily

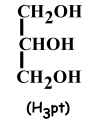

6

afforded [13,30]. To our knowledge there is no other report on the isolation of crystalline vanadate esters of glycerol in the literature.

Determination of representative X-ray structures (see Section 3.2) has revealed that the esters belong to the bonding types **7**–**9** where the three vacant sites are

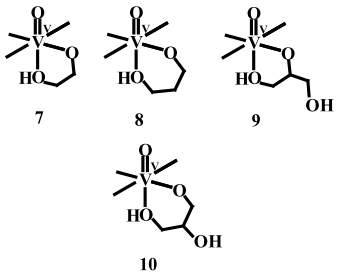

occupied by $Asal^{2-}$ or Abh^{2-}. All the alcohols bind in the monoionized form and the resultant esters are uniformly electroneutral. Interestingly, glycerol binds as a substituted ethane-1,2-diol as in **9** rather than as a substituted propane-1,3-diol as in **10** which is not observed. With characterization of the binding types **7**–**9**, the chelating ability of the two diols as well as of glycerol towards VO^{3+} is firmly authenticated.

3.2. Crystal and molecular structures

The X-ray structures of [V^VO(Hed)(L-psal)] [27], [V^VO(Hed)(L-vsal)] [28], [V^VO(Hpd)(gsal)] [13], [V^VO-(H_2pt)(gsal)] [13], [V^VO(Hed)(babh)] [29], [V^VO-(Hpd)(sabh)] [30] and [V^VO(H_2pt)(sabh)] [30] have been reported. Three representative structures are shown in Figs. 1–3.

The bond lengths within the coordination sphere are set out in Table 1.

In general, the VO_5N coordination sphere is a severely distorted octahedron in which the vanadium atom is displaced by $\sim$0.3 Å from the equatorial plane towards

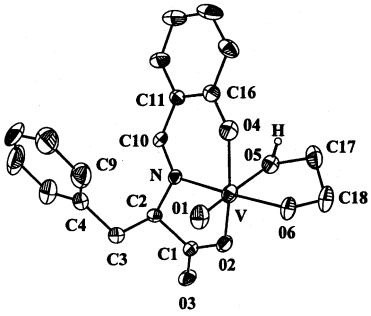

Fig. 1. The structure of [VO(Hed)(L-psal)] [27].

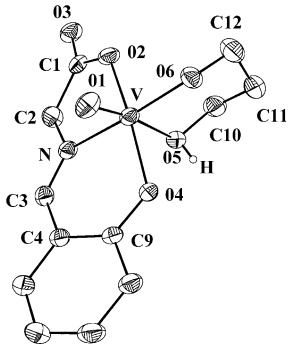

Fig. 2. The structure of [VO(Hpd)(gsal)] [13].

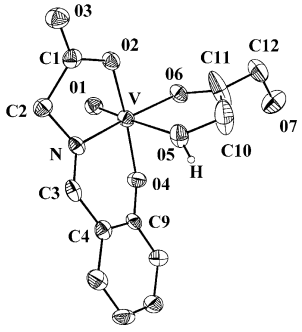

Fig. 3. The structure of [VO(H_2pt)(gsal)] [13].

the oxo-oxygen atom. The five-membered V(Hed) chelate ring is non-planar and the dimethylene bridge has *gauche* configuration. The six-membered V(Hpd) ring has a distorted chair configuration. In phosphate esters the corresponding six-membered ring usually has a boat or twist conformation and the chair is rare [31,32].

The five vanadium–oxygen bonds have different lengths (Table 1) which span the range 1.58–2.33 Å. The shortest is the bond to oxo-oxygen and the longest is that to hydroxyl-oxygen. The remaining bond lengths follow the order V–O (alkoxidic) < V–O (phenoxidic) < V–O (carboxylic/enolic). In some of the structures the alcoholic OH proton was observed directly in difference Fourier maps [13,27,29,30] and

Table 1
Selected bond distances [a] (Å)

	[VO(Hed)(L-psal)]	[VO(Hed)(L-vsal)]	[VO(Hpd)(gsal)]	[VO(H_2pt)(gsal)]
V–O1	1.584(4)	1.581(4)	1.591(3)	1.580(5)
V–O2	1.948(3)	1.948(4)	1.970(3)	1.965(5)
V–O4	1.859(3)	1.866(4)	1.863(3)	1.849(6)
V–O5	2.331(4)	2.320(4)	2.328(3)	2.312(5)
V–O6	1.787(4)	1.794(4)	1.771(3)	1.792(4)
V–N	2.082(4)	2.091(5)	2.098(3)	2.077(6)

[a] Adapted from Refs. [13,27,28].

its presence in all the esters is revealed in IR and ^{1}H-NMR spectra [13,27,28].

In the chiral compounds [V^VO(Hed)(L-psal)] and [V^VO(Hed)(L-vsal)] the signs of atomic coordinates were chosen so as to conform to the *S* configuration of the L-amino acid residue. The residue imposes chiral selectivity on the metal which assumes the configuration in which the V=O axis lies *endo* to the C2–C3 bond (Fig. 1). The *exo* form has not been observed in the solid state but occurs in equilibrium in solution, vide infra.

All the esters display association in the crystalline state due to hydrogen bonding. Thus in [V^VO(Hed)(L-psal)] [27] (as well as [VO(Hed)(L-vsal)] [28]) the alcoholic oxygen of Hed^- and the uncoordinated carboxylate oxygen of a symmetry related molecule associate forming dimers (O···O, 2.760(10) Å). In [V^VO(Hpd)(gsal)] a similar interaction (O···O 2.745(10) Å) results in an infinite chain [13]. In [V^VO(H_2pt)(gsal)] the pendent $-CH_2OH$ oxygen atom of one molecule interlinks alkoxidic and carboxylic oxygen atoms of two adjacent molecules. (O···O, 2.657(13) and 2.611(11) Å) forming a more complex infinite pattern [13]. In the Abh^{2-} esters association involves alcoholic and alkoxidic oxygen atoms as well as the uncoordinated hydrazone nitrogen atom [29,30].

3.3. NMR spectra and solution structure: diastereoisomeric equilibria

Unless otherwise noted the studies of this section refer to the esters with $Asal^{2-}$ coligand. In $(CD_3)_2SO$ solution, the methylene and methine ^{1}H resonances of coordinated Hed^-, Hpd^- and H_2pt^- are systematically shifted to lower fields compared to those of the corresponding free alcohols. In particular, the shift of the bound alkoxide signal can be as large as 2 ppm [13,27]. This has provided a convenient tool for identifying the hydrolysis of the bound alkoxidic ligand. The [VO(Hpd)(Asal)] complexes undergo partial hydrolysis even when the solvent is only slightly wet (~0.5% H_2O). The hydrolysis can be suppressed by adding H_2pd to the solution. The [VO(Hed)(Asal)] and [VO(H_2pt)(Asal)] complexes are much less prone to hydrolysis, and in the same wet solvent as above there is no sign of hydrolysis. Thus the five-membered chelate rings **7** and **9** have superior hydrolytic stability compared to the six-membered ring **8**. The reported difficulty [18–20] in generation of vanadate esters incorporating propane-1,3-diol chelation in aqueous media is thus understandable.

Table 2
^{51}V-NMR spectral data [a] and *K* values in dimethyl-d_6 sulfoxide at 300 K

Compound	δ/ppm [b]	*K*
[VO(Hed)(gsal)]	−531	
[VO(Hed)(L-asal)]	−524 [c], −534 [d]	2.5
[VO(Hed)(L-vsal)]	−525 [c], −535 [d]	31.4
[VO(Hed)(L-psal)]	−522 [c], −535 [d]	3.8
[VO(H_2pt)(gsal)]	−529	
[VO(H_2pt)(L-asal)]	−523 [c], −534 [d]	6.1
[VO(H_2pt)(L-vsal)]	−522 [c], −535 [d]	40.5
[VO(H_2pt)(L-psal)]	−520 [c], −535 [d]	8.3
[VO(Hpd)(gsal)]	−550	
[VO(Hpd)(L-asal)]	−549 [c], −556 [d]	1.7
[VO(Hpd)(L-vsal)]	−547 [c], −556 [d]	10.9
[VO(Hpd)(L-psal)]	−544 [c], −556 [d]	2.3
[VO(Hed)(babh)]	−467	–
[VO(Hed)(sabh)]	−512	–
[VO(H_2pt)(babh)]	−465	–
[VO(H_2pt)(sabh)	−509	–
[VO(Hpd)(babh)]	−496	–
[VO(Hpd)(sabh)]	−538	–

[a] Adapted from Refs. [13,30].
[b] $VOCl_3$ is used as external standard.
[c] *Exo* configuration.
[d] *Endo* configuration.

The ^{51}V-NMR spectra of the complexes are useful in revealing the size of the alkoxy chelate rings and diastereoisomeric equilibria for species having chiral $Asal^{2-}$ ligands. Chemical shift data are listed in Table 2 and representative spectra are shown in Fig. 4 [13]. In the case of the achiral esters of VO(gsal) only a single ^{51}V resonance is observed. In [VO(Hpd)(gsal)] having the six-membered chelate ring **8**, the chemical shift is −550 ppm while in [VO(Hed)(gsal)] having the five-membered chelate ring **7**, it is −531 ppm. Interestingly in the glycerol ester [VO(H_2pt)(gsal)] the shift, −529 ppm, lies close to that of [VO(Hed)(gsal)] and there is no signal near −550 ppm. The glycerol ester thus has the five-membered chelate ring, **9**, in solution as well.

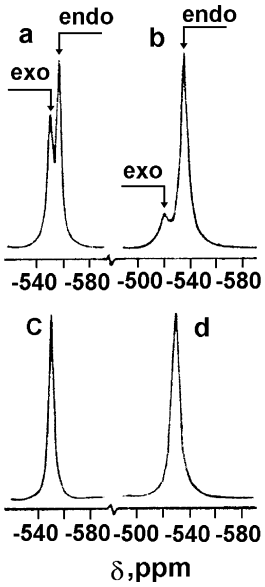

Fig. 4. ^{51}V-NMR spectra of: (a) [VO(Hpd)(L-asal)]; (b) [VO(H_2pt)(L-psal)]; (c)[VO(Hpd)(gsal)]; and (d) [VO(H_2pt)(gsal)] [13].

In the esters with chiral Asal^{2-} ligands two distinct ^{51}V resonances of unequal intensity are generally observed (Table 2). The metal site in the present esters is inherently asymmetric. When Asal^{2-} is chiral, two diastereoisomeric forms are thus possible. These can be conveniently represented as *endo*, **11** and *exo*, **12**. The

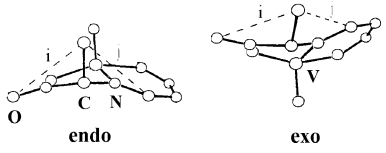

interconversion between **11** and **12** implies inversion of the substitution-labile vanadium site.

The two ^{51}V resonances are assigned to the *endo* **11** and *exo* **12** isomers existing in equilibrium in solution. The stronger signal lying at higher field corresponds to the *endo* form, see below. From the relative intensities of the two resonances the equilibrium constant K, Eq. (1), has been computed (Table 2). The K values are found to

$$K = [endo]/[exo] \quad (1)$$

depend on the Asal^{2-} R group in the order Me < CH_2Ph < $CHMe_2$ and on the alkoxidic chelate ring in the order six-membered < five-membered.

These trends are consistent with steric control, the crucial non-bonded interactions being those of the R group with the uncoordinated carboxyl oxygen atom and the azomethine carbon atom as depicted by the dotted vectors ***i*** and ***j*** in **11** and **12**. These interactions can vary significantly between the *exo* and *endo* configurations because the Asal^{2-} ligand is not planar but has two separate planar regions (OC_6H_4CHN and CCO_2) intersecting along the N–C bond [13,27].

As the R group becomes bulkier the repulsive interaction [13] in the *exo* form increases progressively diminishing the equilibrium concentration of this form. The dihedral angle between the planar parts of the Asal^{2-} ligand is ~10° lower in [VO(Hpd)(gsal)] compared to that in [VO(H_2pt)(gsal)] [13]. The six-membered ester chelate ring is effectively bulkier than the five-membered counterpart tending to flatten the Asal^{2-} ligand and thus decreasing the repulsive interaction in the *exo* configuration. The observed dependence of K on the R group and on the alkoxidic chelate ring size are thus internally consistent.

The ^{51}V-NMR spectra of the hydrazone esters have also been reported [30] and selected chemical shifts are included in Table 2. Each ester displays a single resonance. The effect of the alkoxidic chelate ring size on chemical shift is again evident. The shifts of babh^{2-} esters lie ~40 ppm downfield compared to those of the sabh^{2-} esters.

3.4. Other solution studies: CD spectroscopy and electrochemistry

The chiral VO(Asal) esters display CD spectra [13,27]. In the absorption spectrum an intense band occurs near 340 nm associated with a weaker shoulder near 490 nm. The latter is assigned to O (alkoxy) → V LMCT excitation [33,34]. The presence of strong V ← O (alkoxy) donation is consistent with this assignment. The CD spectrum consists of a well-defined positive peak at 490 nm and a slightly weaker negative peak at 370 nm. Evidently the LMCT excitation has more than one component which is not resolved in the absorption spectrum.

The esters are generally electroactive at platinum in dimethyl sulfoxide solution displaying a quasireversible one-electron response in the range −0.15 to −0.35 V versus SCE [13,27,29,30]. The response is assigned to the $V^{V}O/V^{IV}O$ couple. In the synthesis of the esters from [VO(Asal)(H_2O)] or [VO($acac)_2$] the metal oxidation state increases by one unit ($V^{IV}O \rightarrow V^{V}O$). The oxygen of air can spontaneously act as the oxidizing agent because the metal reduction potentials of the species formed are so low. Alkoxide formation greatly stabilizes the oxovanadium(V) state.

4. Sugar vanadate esters

4.1. Significance, literature and objective

Carbohydrate coordination chemistry is a notable frontier of inorganic research [35,36]. The case of vanadium is particularly interesting because sugar vanadates are potential analogues of sugar phosphates. This enables vanadates to bind enzymes for which the

normal substrates are sugar phosphates or derivatives thereof. Examples are the activation of glucose-6-phosphate dehydrogenase [37] and the inhibition of RNase [8,38] and ATPase [39], as well as the insulin-like function of vanadates [9,10,40].

The usefulness of the ester analogy has in turn prompted research into the sparsely developed chemistry of sugar vanadates [41–48]. Much of the activity has so far been in the solution phase where the presence of complex equilibria have often prevented structurally definitive speciation. The isolation of authentic esters in the pure state has been rare, and both of the two structurally characterized systems are of type **13**, involving alkoxide chelation and bridging promoted by

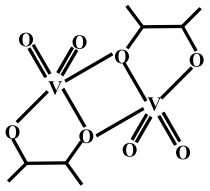

13

diionized sugars—adenosine in one case [49] and a mannopyranoside in the other [50].

The paucity of well characterized sugar vanadates encouraged us to search for new systems using suitably substituted carbohydrates. The design strategy described earlier was used. Species incorporating the binding similar to **7** has been successfully assembled [51–53].

4.2. Methylated hexose and pentose esters with Schiff base coligands

The three sugar ligands (general abbreviation, H_2sug) used are methylated β-D-galactopyranoside (β-D-H_2gp), **14**; α-D-mannopyranoside (α-D-H_2mp), **15**, and β-D-ribofuranoside (β-D-H_2rf), **16**. These were synthesized from the parent glycosides

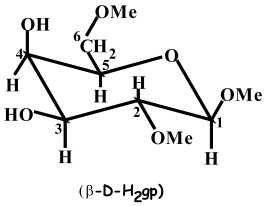

(β-D-H_2gp)

14

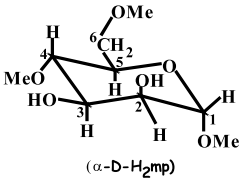

(α-D-H_2mp)

15

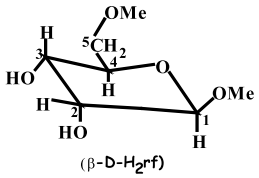

(β-D-H_2rf)

16

via isopropyledene derivative formation, exhaustive methylation followed by hydrolysis [51,53]. Each sugar ligand is so methylated that only two vicinal hydroxyl groups having *cis* disposition (i.e. one axial and the other equatorial) remain free in **14**–**16**. This geometrical feature was introduced so as to facilitate chelation-stabilized ester formation. The schiff base ligands of type H_2Asal, **3** were used to block three coordination positions.

Ester synthesis was achieved as follows. In the case of H_2gsal coligand, a solution of [VO(gsal)(H_2O)] was treated with an excess of H_2sug in methanol in air affording the ester [53]. In case of the other schiff base ligands, [V^VO(Asal)(OMe)(OHMe)] [54,55] was treated with a slight excess of H_2sug in dichloromethane solution followed by layering with *n*-hexane [51].

The esters isolated are listed in Table 3 along with selected characterization data. The sugar hydroxyl stretch is observed near 3200 cm^{-1} as a broad band and the V=O stretch occurs in the range 970–990 cm^{-1}. The red colour of the ester solutions is due to a band occurring near 500 nm assigned to O^-(sugar)→V LMCT excitation. The band is circularly dichroic and CD spectra reveal the presence of overlapping components [51]. The esters display an irreversible, presumably metal-centred ($VO^{3+} \rightarrow VO^{2+}$), reductive voltammetric response in the range −0.2 to −0.3 V (Table 3).

4.3. Crystal and molecular structures

The structures of [VO(β-D-Hgp)(L-vsal)]·H_2O, [VO(α-D-Hmp)(gsal)]·1/2C_6H_6 and [VO(α-D-Hmp)(L-psal)]·H_2O have been reported [51,53]. The asymmetric unit of [VO(β-D-Hgp)(L-vsal)]·H_2O consist of two metrically

Table 3
Selected IR, ^{51}V-NMR and electrochemical data [a]

Compound	IR data [b], ν/cm^{-1}	^{51}V-NMR [c], δ/ppm	$E_{1/2}$, V
[VO(β-D-Hgp)(L-asal)]	980, 3170	−546 [d]	−0.20 [f]
[VO(β-D-Hgp)(L-psal)]	978, 3160	−545 [d]	−0.28 [f]
[VO(β-D-Hgp)(L-vsal)]	975, 3150	−542 [d]	−0.28 [f]
[VO(α-D-Hmp)(gsal)]	985, 3160	−544 [d]	−0.25 [f]
[VO(α-D-Hmp)(L-asal)]	982, 3190	−542 [d]	−0.27 [f]
[VO(α-D-Hmp)(L-psal)]	980, 3170	−543 [d]	−0.25 [f]
[VO(α-D-Hmp)(L-vsal)]	990, 3190	−545 [d]	−0.28 [f]
[VO(β-D-Hrf)(gsal)]	982, 3130	−543 [e]	−0.28 [g]
[VO(β-D-Hrf)(L-asal)]	980, 3160	−544 [e]	−0.28 [g]
VO(β-D-Hrf)(L-psal)	978, 3200	−545 [e]	−0.29 [g]
[VO(β-D-Hrf)(L-vsal)]	972, 3180	−546 [e]	−0.24 [g]

[a] Adapted from Refs. [51,53].
[b] KBr disk.
[c] $VOCl_3$ is used as an external reference.
[d] Solvent is $CDCl_3$.
[e] Solvent is $(CD_3)_2SO$.
[f] Solvent is CH_2Cl_2–MeCN (1:1).
[g] Solvent is Me_2SO.

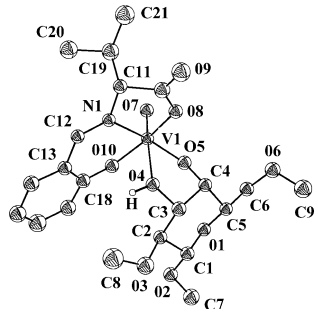

Fig. 5. Perspective view of the molecule 1 in [VO(β-D-Hgp)(L-vsal)]·H_2O (H_2O excluded) [51].

Table 4
Selected bond distances [a] (Å) for [VO(β-D-Hgp)(L-vsal)]·H_2O

Molecule 1		Molecule 2	
V1–O4	2.357(9)	V51–O54	2.297(8)
V1–O5	1.810(9)	V51–O55	1.805(9)
V1–O7	1.585(8)	V51–O57	1.591(8)
V1–O8	1.938(9)	V51–O58	1.946(9)
V1–O10	1.847(9)	V51–O60	1.851(8)
V1–N1	2.084(9)	V51–N51	2.079(10)

[a] Adapted from Ref. [51].

similar but crystallographically distinct molecules and two water molecules. One such molecule is shown in Fig. 5. Bond lengths within the coordination sphere are collected in Table 4 where the numbering of corresponding atoms in molecules 1 and 2 are, respectively, *n* and *n*+50, e.g. V1–O7 and V51–O57. The [VO(α-D-Hmp)(gsal)]·1/2C_6H_6 ester also has two very similar molecules (and a benzene molecule) in the asymmetric unit and one of these is shown in Fig. 6. The bond parameters in the coordination sphere are collected in Table 5. Lastly, [VO(α-D-Hmp)(L-psal)]·H_2O has a single molecule in the asymmetric unit [51].

In each case the monoionized carbohydrate ligand is bonded in the five-membered chelate mode and the alkoxidic and alcoholic oxygen atoms lie *trans* to the azomethine nitrogen atom of $Asal^{2-}$ and the oxo-oxygen atom, respectively. The alcoholic hydrogen

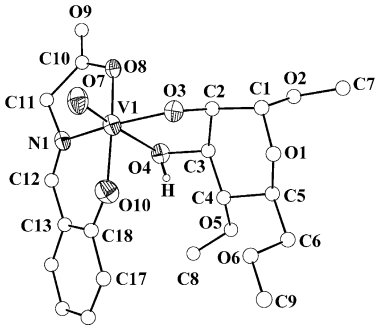

Fig. 6. Perspective view of the molecule 1 in [VO(α-D-Hmp)(gsal)]·1/2C_6H_6 (C_6H_6 excluded) [53].

Table 5
Selected bond distances [a] (Å) for [VO(α-D-Hmp)(gsal)]·1/2C_6H_6

Molecule 1		Molecule 2	
V1–O3	1.799(7)	V51–O53	1.809(6)
V1–O4	2.366(8)	V51–O54	2.325(7)
V1–O7	1.571(7)	V51–O57	1.583(7)
V1–O8	1.970(7)	V51–O58	1.976(6)
V1–O10	1.858(7)	V51–O60	1.863(7)
V1–N1	2.072(8)	V51–N51	2.063(8)

[a] Adapted from Ref. [53].

atom was directly observed in difference Fourier maps in all three esters. In the carbohydrate framework the alkoxide and alcohol functions respectively occupy axial and equatorial positions in both [VO(β-D-Hgp)(L-vsal)]·H_2O (both molecules) and [VO(α-D-Hmp)(gsal)]·1/2C_6H_6 (both molecules). In [VO(α-D-Hmp)(L-psal)]·H_2O the disposition is reversed [51].

The geometry of the VO_5N coordination sphere is similar to that in the esters of diols and the V–O bond lengths follow similar trends. The anomeric configuration of each sugar ligand is preserved in the esters. In the cases of the two esters with chiral $Asal^{2-}$ ligands the observed geometry is *endo* [51].

The water molecules in both the two hydrated esters are involved in strong hydrogen bonding. In [VO(β-D-Hgp)(L-vsal)]·H_2O the two ester molecules of the asymmetric unit along with the water molecules constitute a macrocyclic supramolecule held by alcohol···water (O···O, 2.586(12) Å), water···water (2.863(14) Å), water···ether (2.840(13) Å), and alcohol···ether (2.660(12) Å) hydrogen bonds (Fig. 7). The approximate diameter of the macrocyclic cavity is 6.1 Å. In [VO(α-D-Hmp)(L-psal)]·H_2O each water molecule bridges two symmetry-related ester molecules via alkoxide···water and alcohol···water hydrogen bonds of O···O lengths 2.850(11) and 2.647(10) Å, respectively, resulting in an infinite chain structure [51]. In [VO(α-D-Hmp)(gsal)]·1/2C_6H_6, molecules 1 and 2 are linked into a dimer via carboxylate···alcohol hydrogen bonds of O···O lengths 2.698(12) and 2.638(11) Å. The average cavity diameter of the macrocycle so formed is 4.5 Å [53].

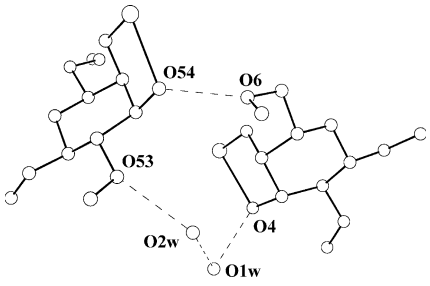

Fig. 7. Hydrogen bonding in [VO(β-D-Hgp)(L-vsal)]·H_2O [51].

4.4. Solution structure

The solid state structures are preserved in solutions as revealed by ^{1}H- and ^{51}V-NMR spectroscopy [51,53]. No isomerization is detectable either at the metal site or at the anomeric carbon site. Further, the mode of metal–carbohydrate binding remains unaltered. Also each ester displays a single ^{51}V line near −545 ppm (Table 3) assignable to the *endo* isomer (for esters with chiral $Asal^{2-}$). There is no diastereoisomeric splitting of the ^{1}H resonances. The chiral preference at the metal site is more strongly expressed in the carbohydrate esters than

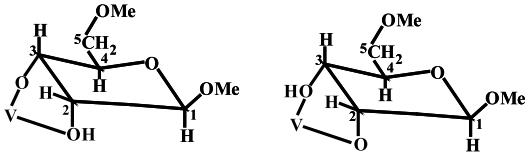

17 18

in Hed^{-} and H_2pt^{-} esters where the *exo* isomer is observed as a minor constituent. The ^{1}H-NMR spectra of the [VO(α-D-Hrf)(Asal)] esters (which did not afford single crystals) are consistent with the bonding mode **17** as opposed to **18** [53].

4.5. A pentacoordinated mannopyranoside ester with a hydrazone coligand

The concerned sugar is 4,6-benzylidine-α-D-manno-pyranoside (α-D-H_2bmp), **19** which has been shown earlier to furnish alkoxide bridged dimeric esters of VO_2^{+} [50]. The reaction of this sugar with [V^{V}O(sabh)-

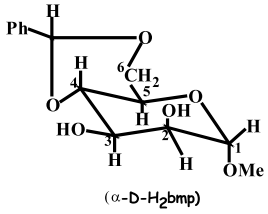

(α-D-H_2bmp)

19

(OMe)(OHMe)] [29] in methanol afforded the ester [VO(α-D-Hbmp)(sabh)] as a dark coloured crystalline solid in excellent yields [56]. The V=O and OH stretches occur at 980 and 3185 cm^{-1}, respectively. The $VO^{3+} \rightarrow VO^{2+}$ reduction occurs at −0.10 V versus SCE in CH_2Cl_2 solution.

The X-ray structure of the ester is shown in Fig. 8 and selected bond parameters are listed in Table 6. A notable feature of the present ester is the long V···O (alcoholic) contact, 2.514(5) Å, signifying the virtual absence of bonding. In effect, [VO(α-D-Hbmp)(sabh)] is a square-pyramidal ester. Since the V=O length is normal, the state of V···O (alcoholic) contact cannot be ascribed to any augmented *trans* influence. It arises from changes in carbohydrate bond parameters [56]. The alcoholic O4

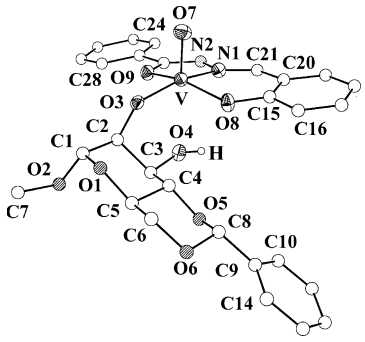

Fig. 8. The structure of [VO(α-D-Hbmp)(sabh)] [56].

Table 6
Selected bond distances [a] (Å) for [VO(α-D-Hbmp)(sabh)]

V–O3	1.795(4)	V–O7	1.592(5)
V–O8	1.839(4)	V–O9	1.918(4)
V–N1	2.084(6)		

[a] Adapted from Ref. [57].

atom is engaged in intermolecular hydrogen bonding with the oxo-oxygen O7 (O4···O7, 2.918(10) Å) generating a helical pattern parallel to the b axis, Fig. 9. This mode of hydrogen bonding is distinct from those observed in the sugar vanadates of type [VO(Hsug)(Asal)] [51,53].

The vanadium site in the ester is chiral. Viewing down the V=O axis and using the priority sequence O9 > O8 > O3 > N1 for the equatorial atoms, the observed configuration is *A* (anticlockwise) [57]. There is no evidence that the diastereoisomer incorporating the *C* configuration exists either in the solid state or in solution. Model building reveals the presence of serious interference between the pendent phenyl ring of $sabh^{2-}$ and α-D-$Hbmp^{-}$ ligands in the unobserved diastereoisomer.

In $CDCl_3$, the ester displays a single sharp ^{51}V-NMR line (−539 ppm) as well as a single ^{1}H NMR feature for each type of proton (no diastereoisomers). The alcoholic

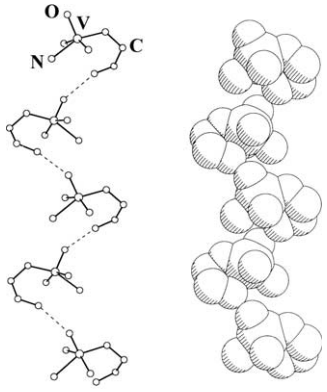

Fig. 9. Hydrogen bonding in crystalline [VO(α-D-Hbmp)(sabh)] in ball-and-stick and space-filling forms [56].

OH group gives rise to a relatively broad ^{1}H signal at 5.92 ppm. Interestingly in [VO(Hsug)(Asal)] species where there is significant V–OH interaction, the OH signal is shifted down field to ~7.2 ppm [51,53].

5. Esters of aromatic 1,2-diols (catechols)

5.1. Synthesis and characterization

Colour reactions of vanadium with catechols have long been used in analytical chemistry and the species formed have been attracting the attention of solution and structural chemists for some time [58–62]. Among structurally characterized [58,63–72] diphenol complexes of vanadium the usual binding mode is **20**. The successful design of mononuclear esters with ethane-1,2-

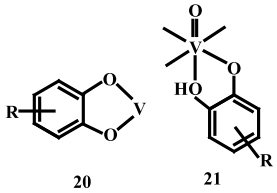

20 21

diol and carbohydrates encouraged us to explore the feasibility of binding catechols to oxovanadium(V) in the form **21**. This has been achieved using the hydrazones H_2sabh, and H_2Clsabh (**5**) as blocking coligands [73–75].

The two 1,2-diphenols (general abbreviation H_2dp) studied are **22** and **23**. Chelation of type **21** could be achieved by using three synthetic routes: the reaction of

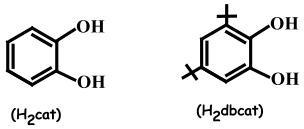

(H_2cat) (H_2dbcat)

22 23

[VO(Abh)(OMe)(OHMe)] with excess H_2dp in MeOH; the reaction of [VO(acac)$_2$] with H_2Abh in MeOH/Me_2CO/CH_2Cl_2 in air (oxidant is O_2) in the presence of H_2dp and the reaction of dimeric [V_2O_3(Abh)$_2$] [73–76] with excess H_2dp in CH_2Cl_2/Me_2CO.

Three esters and their selected spectral properties are listed in Table 7. The red coloured aliphatic esters described earlier absorb weakly near 500 nm (O^-(alkoxide)→V LMCT) but the present aromatic esters are blue to blue–violet in colour absorbing strongly near 600 nm (O^- (phenoxide)→V LMCT). The ^{1}H-NMR spectra of the species are as expected [73–75] and the phenolic OH function is observed as a broad signal (11.4–11.5 ppm). The ^{51}V resonances occur ~200 ppm downfield compared to those of the aliphatic species presumably due to contribution of charge transfer states to the ground level [72]. In CH_2Cl_2 (2% MeCN) the esters display complex voltammograms with a cathodic peak in the range −0.3–0.0 V (metal reduction) and one or two anodic peaks above 0.5 V (Hdp^- oxidation) [74].

5.2. Crystal and molecular structure

The structure of [VO(Hdbcat)(sabh)] is shown in Fig. 10 and selected bond parameters are given in Table 8. The five unequal V–O bond lengths follow the order: O(1)(oxo) ≪ O(5) (phenoxy, $Hdbcat^-$) < O(2) (phenoxy, $sabh^{2-}$) < O(3) (enolate, $sabh^{2-}$) ≪ O(4) (phenolic, $Hdbcat^-$). The phenolic hydrogen atom of $Hdbcat^-$ was observed in difference Fourier maps. This is the first authentication of chelation by a monoionized catechol in vanadium complexes. Such chelation is generally rare for any metal, but has been documented in an iron(II) complex [77]. In the lattice the ester molecules form dimers due to intermolecular N2···O4 hydrogen bonds of lengths 2.662(8) Å.

5.3. Reaction with oxygen: catecholase activity

The oxidation of catechols to quinones by O_2—the catecholase reaction—is an important biochemical transformation usually catalysed by binuclear copper [78–80]. It has been found that the [VO(Hdp)(Abh)] esters cleanly promote the catecholase reaction [73,74]. The esters are stable in the solid state in air and their blue solutions (CH_2Cl_2/MeCN/Me_2CO) are also perfectly stable both in terms of redox and dissociation but

Table 7
Selected IR, ^{51}V-NMR and electronic spectra data [a]

Compound	IR data [b], ν/cm^{-1}	UV–vis[c], λ_{max}/nm (ε, M^{-1}, cm^{-1})	^{51}V-NMR [d,e] (δ/ppm)
[VO(Hcat)(sabh)	995, 3410	550(4730), 410(5540)	−430
[VO(Hdbcat)(sabh)	990, 3450	600(7410), 400(8230)	−371
[VO(Hdbcat)(Clsabh)	985, 3425	610(7640), 415(5980)	−350

[a] Adapted from Ref. [73].
[b] KBr disk/halocarbon mull.
[c] Solvent is acetone.
[d] In $(CD_3)_2CO$.
[e] $VOCl_3$ is used as an external reference.

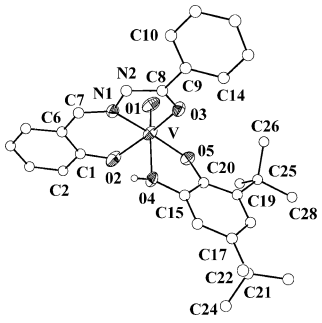

Fig. 10. The structure of [VO(Hdbcat)(sabh)] [73].

Table 8
Selected bond distances [a] (Å) for [VO(Hdbcat)(sabh)]

V–O1	1.582(4)	V–O4	2.344(4)
V–O2	1.857(4)	V–O5	1.811(4)
V–O3	1.945(4)	V–N1	2.091(5)

[a] Adapted from Ref. [73].

only under N_2/Ar. In the presence of O_2, the solution colour progressively changes, finally becoming yellowish-red. The original colour is fully reestablished upon adding the relevant catechol externally. A second cycle of reaction with oxygen can then begin proceeding in the same way as above. In this way many cycles can be completed with retention of the reactivity of [VO(Hdp)(Abh)] at the original level. In the case of [VO(Hdbcat)(sabh)], the products quantitatively isolated are dbq, **24** and $[V_2O_3(sabh)_2]$. The catalytic cycle of Fig. 11 is thus operative. Here the catalyst is $[V_2O_3(sabh)_2]$ and

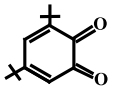

(dbq)

24

the ester is the reactive intermediate. The net result of the

$$H_2dbcat + 1/2O_2 \rightarrow dbq + H_2O \quad (2)$$

cycle is the catecholase reaction, Eq. (2). Careful ^{1}H-NMR studies of reacting solutions have revealed that the quinone is the only product of oxidation of the ester [73]. In reported oxidations of catechols by oxygen in the presence of vanadium complexes, the major product is generally muconic acid anhydride along with some quinone and 2-pyrone [62,81,82].

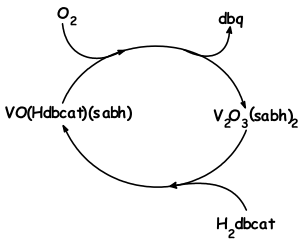

Fig. 11. Catalytic cycle based on catecholase reaction of [VO(Hdbcat)(sabh)] [73].

Spectrophotometric rate studies in O_2-saturated Me_2CO at 295 K have afforded the following pseudo-first-order rate constants of the oxidation process: [VO(Hdbcat)(sabh)], 4.50×10^{-4} s^{-1}; [VO(Hdbcat)(Cl-sabh)], 2.80×10^{-4} s^{-1} and [VO(Hcat)(sabh)], 1.10×10^{-4} s^{-1}. Thus electron withdrawal from either the catecholate ligand or the hydrazone coligand diminishes k_{obs}, clearly implying that electron transfer to O_2 occurs from the intact complex and not from dissociated catechol ligand.

A plausible mode of O_2 attachment is stylized in **25**. Attachment of O_2 via hydrogen bridging has been implicated in e.g. hemoglobin [83,84] and hemerythrin [85] chemistry. Electron transfer from the catecholate in

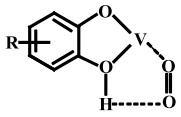

25

25 to O_2 may occur via the hydrogen bond or the metal or both. There is no direct evidence that the metal site is involved. The reacting solutions do not display any EPR signals either in fluid or in frozen conditions due to $V^{IV}O$ intermediates. Periodic examination of aqueous extracts of reacting solutions with O_2-sensitive electrodes for liberation of O_2 upon addition of peroxidase enzyme gave negative result. Thus O_2 appears to be reduced to H_2O without the intermediacy of H_2O_2.

Esters of type [VO(Hdp)(Asal)] have been successfully isolated and their catecholase activity is under scrutiny [75].

Acknowledgements

The authors are grateful to Indian National Science Academy, New Delhi, Department of Science and Technology, New Delhi and Council of Scientific and Industrial Research, New Delhi for Financial support. They are thankful to Dr S. Mondal, Dr S.P. Rath and Dr K.K. Rajak for help.

References

[1] W. Prandtl, L.Z. Hess, Z. Anorg. Chem. 82 (1913) 103.
[2] A.J. Blair, D.A. Pantony, G.J. Minkoff, J. Inorg. Nucl. Chem. 5 (1958) 316.
[3] F. Cartan, C.N. Caughlan, J. Phys. Chem. 64 (1960) 1756.
[4] C.N. Caughlan, H.M. Smith, K. Watenpaugh, Inorg. Chem. 5 (1966) 2131.
[5] W. Priebsch, D. Rehder, Inorg. Chem. 29 (1990) 3013.

[6] F. Hillerns, F. Olbrich, U. Beherm, D. Rehder, Angew. Chem. Int. Ed. Engl. 31 (1992) 447.
[7] D.C. Crans, H. Chen, R.A. Felty, J. Am. Chem. Soc. 114 (1992) 4543.
[8] R.N. Lindquist, J.L. Lynn, Jr., G.E. Leinhard, J. Am. Chem. Soc. 95 (1973) 8762.
[9] B.I. Posner, R. Faure, J.W. Burgess, A.P. Bevan, D. Lachance, G. Zhang-Sun, I.G. Fantus, J.B. Ng, D.A. Hall, B. Soo Lum, A. Shaver, J. Biol. Chem. 269 (1994) 4596.
[10] P.J. Stankiewicz, A.S. Tracey, D.C. Crans, in: H. Sigel, A. Sigel (Eds.), Metal Ions in Biological Systems, Marcel Dekker, New York, 1995, p. 287.
[11] D. Rehder, Angew. Chem. Int. Ed. Engl. 30 (1991) 148.
[12] D.C. Crans, in: H. Sigel, A. Sigel (Eds.), Metal Ions in Biological Systems, Marcel Dekker, New York, 1995, p. 147.
[13] S. Mondal, S.P. Rath, K.K. Rajak, A. Chakravorty, Inorg. Chem. 37 (1998) 1713.
[14] M.J. Gresser, A.S. Tracey, J. Am. Chem. Soc. 108 (1986) 1935.
[15] W.J. Ray, Jr., D.C. Crans, J. Zheng, J.W. Burgner, II, H. Deng, M. Mahroof-Tahir, J. Am. Chem. Soc. 117 (1995) 6015.
[16] D.C. Crans, R.A. Felty, O.P. Anderson, M.M. Miller, Inorg. Chem. 32 (1993) 247.
[17] D.C. Crans, R.A. Felty, H. Chen, H. Eckert, N. Das, Inorg. Chem. 33 (1994) 2427.
[18] A.S. Tracey, M.J. Gresser, Inorg. Chem. 27 (1988) 1269.
[19] A.S. Tracey, M.J. Gresser, Can. J. Chem. 66 (1988) 2570.
[20] D.C. Crans, R.W. Marshman, M.S. Gottlieb, O.P. Anderson, M.M. Miller, Inorg. Chem. 31 (1992) 4939.
[21] J. Chakravarty, S. Dutta, S.K. Chandra, P. Basu, A. Chakravorty, Inorg. Chem. 32 (1993) 4249.
[22] J. Chakravarty, S. Dutta, Aparna Dey, A. Chakravorty, J. Chem. Soc. Dalton Trans. (1994) 557.
[23] S. Mondal, S. Dutta, A. Chakravorty, J. Chem. Soc. Dalton Trans. (1995) 1115.
[24] A.K. Mukherjee, P. Ray, J. Indian Chem. Soc. 32 (1955) 505.
[25] R. Hamalainen, U. Turpeinen, M. Ahlgren, Acta Crystallogr. Sect. C 41 (1985) 1726.
[26] L.J. Theriot, G.O. Carlisle, H.J. Hu, J. Inorg. Nucl. Chem. 31 (1969) 2841.
[27] S. Mondal, S.P. Rath, S. Dutta, A. Chakravorty, J. Chem. Soc. Dalton Trans. (1996) 99.
[28] S. Mondal, P. Ghosh, A. Chakravorty, Indian J. Chem. Sect. A 35 (1996) 171.
[29] S.P. Rath, S. Mondal, A. Chakravorty, Inorg. Chim. Acta 263 (1997) 247.
[30] S.P. Rath, K.K. Rajak, S. Mondal, A. Chakravorty, J. Chem. Soc. Dalton Trans. (1998) 2097.
[31] Y. Huang, A.M. Arif, W.G. Bentrude, J. Am. Chem. Soc. 113 (1991) 7800.
[32] J. Hans, R.O. Day, R.R. Holmes, Inorg. Chem. 30 (1991) 3928.
[33] C.J. Carrano, M. Mohan, S.M. Holmes, R. de la Rosa, A. Butler, J.M. Charnock, C.D. Garner, Inorg. Chem. 33 (1994) 646.
[34] J.M. Arber, E. de Boer, C.D. Garner, S.S. Hasnain, R. Wever, Biochemistry 28 (1989) 7968.
[35] U. Piarulli, C. Floriani, Prog. Inorg. Chem. 45 (1997) 393.
[36] J. Verchere, S. Chapelle, F. Xin, D.C. Crans, Prog. Inorg. Chem. 47 (1998) 837.
[37] A.F. Nour-Eldeen, M.M. Craig, M.J. Gresser, J. Biol. Chem. 260 (1985) 6836.
[38] B. Borah, C.W. Chen, W. Egan, M. Miller, A. Wlodawer, J.S. Chohen, Biochemistry 24 (1985) 2058.
[39] N.D. Chasteen (Ed.), Vanadium in Biological System: Physiology and Biochemistry, Kluwer, Dordrecht, 1990, p. 153.
[40] C. Slebodnick, B.J. Hamstra, V.L. Pecoraro, Metal Sites in Proteins and Models, Springer, Berlin, Germany, 1999, p. 69.
[41] A.S. Tracey, M.J. Gresser, Inorg. Chem. 27 (1988) 2695.
[42] A.S. Tracey, C.H. Leon-Lai, Inorg. Chem. 30 (1991) 3200.
[43] X. Zhang, A.S. Tracey, Acta Chem. Scand. 46 (1992) 1170.
[44] D.C. Crans, S.E. Harnung, E. Larsen, L.A. Theisen, I. Trabjerg, Acta Chem. Scand. 45 (1991) 456.
[45] C.F.G.C. Geraldes, M.M.C.A. Castro, J. Inorg. Biochem. 35 (1989) 79.
[46] J. Richter, D. Rehder, L. Wyns, A. Haikal, Inorg. Chim. Acta 238 (1995) 115.
[47] J. Richter, D. Rehder, Z. Naturforsch. Teil. B 46 (1991) 1613.
[48] A. Sreedhara, C.P. Rao, B. Rao, J. Carbohydr. Res. 289 (1996) 39.
[49] S.J. Angus-Dunne, R.J. Batchelor, A.S. Tracey, F.W.B. Einstein, J. Am. Chem. Soc. 117 (1995) 5292.
[50] B. Zhang, S. Zhang, K. Wang, J. Chem. Soc. Dalton Trans. (1996) 3257.
[51] K.K. Rajak, S.P. Rath, S. Mondal, A. Chakravorty, Inorg. Chem. 38 (1999) 3283.
[52] K.K. Rajak, S.P. Rath, S. Mondal, A. Chakravorty, Indian J. Chem. Sect. A 38 (1999) 405.
[53] K.K. Rajak, S.P. Rath, S. Mondal, A. Chakravorty, J. Chem. Soc. Dalton Trans. (1999) 2537.
[54] K. Nakajima, M. Kojima, K. Toriumi, K. Saito, J. Fujita, Bull. Chem. Soc. Jpn. 62 (1989) 760.
[55] S. Dutta, S. Mondal, A. Chakravorty, Polyhedron 14 (1995) 1163.
[56] K.K. Rajak, B. Baruah, S.P. Rath, A. Chakravorty, Inorg. Chem. 39 (2000) 1598.
[57] G.J. Leigh (Ed.), Nomenclature of Inorganic Chemistry, Blackwell Scientific Publication, Oxford, 1990, p. 182.
[58] S.R. Cooper, Y.B. Koh, K.N. Raymond, J. Am. Chem. Soc. 104 (1982) 5092.
[59] R.P. Henry, P.C. Mitchell, J.E. Prue, J. Chem. Soc. Dalton Trans. (1973) 1156.
[60] P.J. Bosserman, D.T. Sawyer, Inorg. Chem. 21 (1982) 1545.
[61] Y. Tatsuno, M. Tatsuda, S. Otsuka, J. Chem. Soc. Chem. Commun. (1982) 1100.
[62] C.G. Pierpont, C.W. Lange, In: K.D. Karlin (Ed.), Progress in Inorganic Chemistry, vol. 41, Interscience, New York, 1994, p. 331.
[63] M.E. Cass, D.L. Greene, R.M. Buchanan, C.G. Pierpont, J. Am. Chem. Soc. 105 (1983) 2680.
[64] A.R. Bulls, C.G. Pippin, F.E. Hahn, K.N. Raymond, J. Am. Chem. Soc. 112 (1990) 2627.
[65] S. Lee, K. Nakanishi, M.Y. Chiang, R.B. Frankel, K. Spartalian, J. Chem. Soc. Chem. Commun. (1988) 785.
[66] M. Mazzanti, C. Floriani, A. Chiesi-Villa, C. Guastini, J. Chem. Soc. Dalton Trans. (1989) 1793.
[67] C.L. Simpson, C.G. Pierpont, Inorg. Chem. 31 (1992) 4308.
[68] T.A. Kabanos, A.J.P. White, D.J. William, J.D. Woolins, J. Chem. Soc. Chem. Commun. (1992) 17.
[69] T.M. Dewey, J.D. Bois, K.N. Raymond, Inorg. Chem. 32 (1993) 1729.
[70] M.E. Cass, N.R. Gordon, C.G. Pierpont, Inorg. Chem. 25 (1986) 3962.
[71] T.A. Kabanos, A.M.Z. Slawin, D.J. Williams, J.D. Woollins, J. Chem. Soc. Chem. Commun. (1990) 193.
[72] C.R. Cornman, G.J. Colpas, J.D. Hoeschele, J. Kampt, V.L. Pecoraro, J. Am. Chem. Soc. 114 (1992) 9925.
[73] S.P. Rath, K.K. Rajak, A. Chakravorty, Inorg. Chem. 38 (1999) 4376.
[74] S.P. Rath, Ph.D. Thesis, Jadavpur University, Jadavpur, Kolkata, India, 1998.
[75] B. Baruah, S. Das, A. Chakravorty, Inorg. Chem. 41 (2002) 4502.
[76] N.R. Sangeetha, S. Pal, Bull. Chem. Soc. Jpn. 73 (2000) 357.
[77] L. Shu, Y.M. Chiou, A.M. Orville, M.A. Miller, J.D. Lipscomb, L. Que, Jr., Biochemistry 34 (1995) 6649.

[78] K.D. Karlin, Z. Tyeklar (Eds.), Bioinorganic Chemistry of Copper, Chapman and Hall, New York, 1993, p. 184.
[79] E.I. Solomon, M.J. Baldwin, M.D. Lowery, Chem. Rev. 92 (1992) 521.
[80] N. Kitajima, Y. More-Oka, Chem. Rev. 94 (1994) 737.
[81] U. Casellato, S. Tamburini, P.A. Vigato, M. Vidali, D.E. Fenton, Inorg. Chim. Acta 84 (1984) 101.
[82] B. Galeffi, M. Postel, A. Grand, P. Rey, Inorg. Chim. Acta 160 (1989) 87.
[83] M.F. Perutz, G. Fermi, B. Luisi, B. Shaanan, R.C. Liddington, Acc. Chem. Res. 20 (1987) 309.
[84] B. Shaanan, J. Mol. Biol. 171 (1983) 31.
[85] R.E. Stenkamp, Chem. Rev. 94 (1994) 715.